

ACCURACY ANALYSIS OF ROTOR FREQUENCY CALCULATION FOR INDUCTION MOTOR DRIVE

Tomáš Lažek

Doctoral Degree Programme (2), FEEC BUT

E-mail: xlazek00@stud.feec.vutbr.cz

Supervised by: Ivo Pazdera

E-mail: pazderai@feec.vutbr.cz

Abstract: This paper deals with the accuracy analysis of rotor frequency calculations for an analytical formula of the optimal linkage flux. First, an equivalent circuit of the induction machine and a loss model are described. Furthermore, the calculation of the rotor frequency is performed for two cases, which are compared. The results show that the rotor frequency can be calculated in a simplified form without a large difference in accuracy.

Keywords: accuracy analysis, induction motor, loss minimization, variable speed drive

1 INTRODUCTION

In recent years, there has been an emphasis on reducing electricity consumption. The largest consumers of electricity are variable speed electric drives. Here is a great opportunity to reduce the consumption of electric drives by using an algorithm to increase the efficiency of the electric drive.

The efficiency of the drive can be controlled by an adaptive regulator, which reduces the value of the linkage flux, thus reducing losses. One of the commonly used strategies is model-based method which requires the loss model of the induction motor [1].

The goal of this paper is to determine the difference between the two methods of calculating rotor frequency. Both calculation methods are compared with each other. The influence of other parameters such as stator currents and power losses are compared. The conclusion evaluates the influence of both calculations on the parameters accuracy necessary for the operation of the regulator.

2 INDUCTION MACHINE MODEL

An equivalent circuit in the form of a commonly used gamma network is used. The resistor representing the iron resistance is connected parallel to the magnetization inductance. Detailed development of the model can be found [2]. The steady-state model shown in Figure 1 is defined in the rotating (d,q) stator flux frame. Thus $\Psi_{sd} = \Psi_s$ and $\Psi_{sq} = 0$.

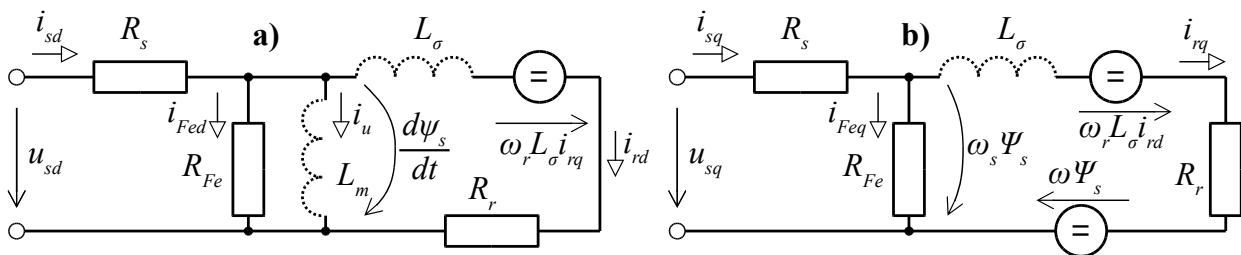


Figure 1: Steady-state induction machine equivalent circuit in: a) d-axis and b) q-axis.

In the steady-state model, the coils can be thought of as a short circuit. The stator voltage u_{sd} and u_{sq} is given as:

$$u_{sd} = R_s \cdot i_{sd} \quad (1)$$

$$u_{sq} = R_s i_{sq} + \omega_s \psi_s \quad \omega_s \psi_s = \omega_r L_\sigma i_{rd} + R_r i_{rq} + \omega \psi_s \quad (2a, b)$$

where ω_r is the difference between the synchronous frequency ω_s and the mechanical speed ω . The synchronous frequency ω_s can be expressed as the mechanical speed ω multiplied by the number of pole-pairs p . The currents i_{sd} and i_{sq} in the model are described as follows:

$$i_{sd} = i_u + i_{rd} \quad i_u = \frac{\psi_s}{L_m} \quad i_{rd} = \frac{\omega_r L_\sigma i_{sq}}{R_r} \quad (3a, b, c)$$

$$i_{rq} = i_{sq} - i_{Feq} = i_{sq} \quad i_{sq} = \frac{2T}{3p\psi_s} \quad (4a, b)$$

The current i_{Feq} and i_{Fed} can be considered as zero, because the resistance R_{Fe} is many times greater than the resistance R_r . It is advantageous to express the current i_{sq} in terms of torque and stator linkage flux. Furthermore, from the Figure 1 follows that the voltage at R_{Fe} is determined by the voltage $\omega_s \psi_s$.

3 LOSS MODEL

The loss model of an induction motor is advantageous to express depending on the mechanical speed, torque, and linkage flux. The aim is to obtain an analytical expression for the optimal linkage flux at a given torque and known shaft speed. However, the formula compilation is not within the scope of this article.

The parameter R_{Fe} must not be constant due to the loss model accuracy. The iron losses consist of losses by eddy currents and hysteresis losses. According to [2], both resistance values can be combined to create a simple linear dependence of the total iron resistance on frequency.

$$R_{Fe} = R_{Fe0} \frac{\omega_s}{\omega_{s0}} \quad (5)$$

The iron resistance R_{Fe0} must be determined at the specified frequency ω_{s0} .

Determining stator Joule losses P_{js} in the substitution model in d-q axis is very simple. The resistance of the stator winding R_s is multiplied by the square of the current flowing through it. It can be seen from Figure 2 that both i_{sd} and i_{sq} flow through the resistor R_s . The determination of Joule losses in the rotor P_{jr} is similar to the difference that the rotor currents i_{rd} and i_{rq} flow through the resistor R_r . As mentioned above, $i_{rq} = i_{sq}$. Thus:

$$P_{js} = R_s(i_{sd}^2 + i_{sq}^2) \quad P_{jr} = R_r(i_{rd}^2 + i_{sq}^2) \quad (6a, b)$$

4 CALCULATION OF ROTOR FREQUENCY

For calculation current i_{rd} , it is necessary to know rotor frequency ω_r . The rotor frequency can be expressed from equation (2b) as follows:

$$\omega_r \psi_s = \omega_r L_\sigma i_{rd} + R_r i_{sq} \quad (7)$$

To simplify the expression, the $L_\sigma \omega_s \cdot i_{rd}$ can be neglected due to the small rotor current in the d-axis. Then ω_r with aid of (4b) may be written as:

$$\omega_{rA} = \frac{2R_r T}{3p\psi_s^2} \quad (8)$$

Then the currents in the d-axis can be expressed:

$$i_{rdA} = \frac{4T^2 L_\sigma}{9p^2 \psi_s^3} \quad i_{sdA} = \frac{\psi_s}{L_m} + \frac{4T^2 L_\sigma}{9p^2 \psi_s^3} \quad (9a, b)$$

The natural solution of equation (7) leads to a quadratic equation:

$$\omega_{rB} = \frac{3p\psi_s^2 \pm \sqrt{9p^2 \psi_s^4 + 16p^2 L_\sigma^2}}{4T L_\sigma^2 / R_r} \quad (10)$$

Only the negative sign can be taken into account. A positive sign represents operate with high slip before the pull-out torque of the torque characteristic, which is undesirable.

Then the currents in the d-axis can be expressed as follows:

$$i_{rdB} = \frac{2T}{3p\psi_s} \frac{3p\psi_s^2 - \sqrt{9p^2 \psi_s^4 + 16p^2 L_\sigma^2}}{4T L_\sigma} \quad i_{sdB} = \frac{\psi_s}{L_m} + \frac{2T}{3p\psi_s} \frac{3p\psi_s^2 - \sqrt{9p^2 \psi_s^4 + 16p^2 L_\sigma^2}}{4T L_\sigma} \quad (11a, b)$$

5 ACCURACY VERIFICATION OF ROTOR FREQUENCY CALCULATIONS

The aim of this chapter is to verify the accuracy of the calculation of currents and losses in the motor when considering the simplified expression for ω_r (8) and when considering the natural expression for ω_r (10) for

different values of linkage flux. It should be noted that at reduced flux, no permanent load with nominal torque is expected. The value of ω_r according to the equation (10) is limited only to the value of the pull-out torque, which can be expressed from the condition for the square root of the expression (10). It can be seen from this equation that the pull-out torque decreases with decreasing linkage flux.

Verification was performed in MATLAB environment with the parameters of the real induction motor. Since the determination of parameters is not the subject of this article, the values of the required rated parameters of induction motor ATAS T22VR512 are: torque $T_n = 2\text{Nm}$, speed $n_n = 2380\text{ min}^{-1}$, linkage flux (peak) $\Psi_n = 1\text{ Vs}$, number of pole-pairs $p = 1$; stator resistance $R_s = 11.8\ \Omega$, rotor resistance $R_r = 9.2\ \Omega$, iron loss resistance $R_{Fe}(50\text{ Hz}) = 4900\ \Omega$, leakage inductance $L_\sigma = 90\text{ mH}$. Magnetization inductance is a function of the linkage flux, and its values are: $L_m(\Psi = 1\text{ Vs}) = 0.9\text{ H}$, $L_m(\Psi = 1.1\text{ Vs}) = 0.7\text{ H}$, $L_m(\Psi = 0.75\text{ Vs}) = 1.07\text{ H}$, $L_m(\Psi = 0.5\text{ Vs}) = 1.2\text{ H}$. Details of the parameters of the induction motor are given in [3].

Figure 2 shows the difference of the values of ω_r according to equations (8) and (10) as a function of the torque for four linkage flux values. It can be seen that at rated linkage flux $\psi = 1\text{ Vs}$ the difference between the values ω_{rA} and ω_{rB} is negligible to the rated torque. This difference increases at higher torques than the

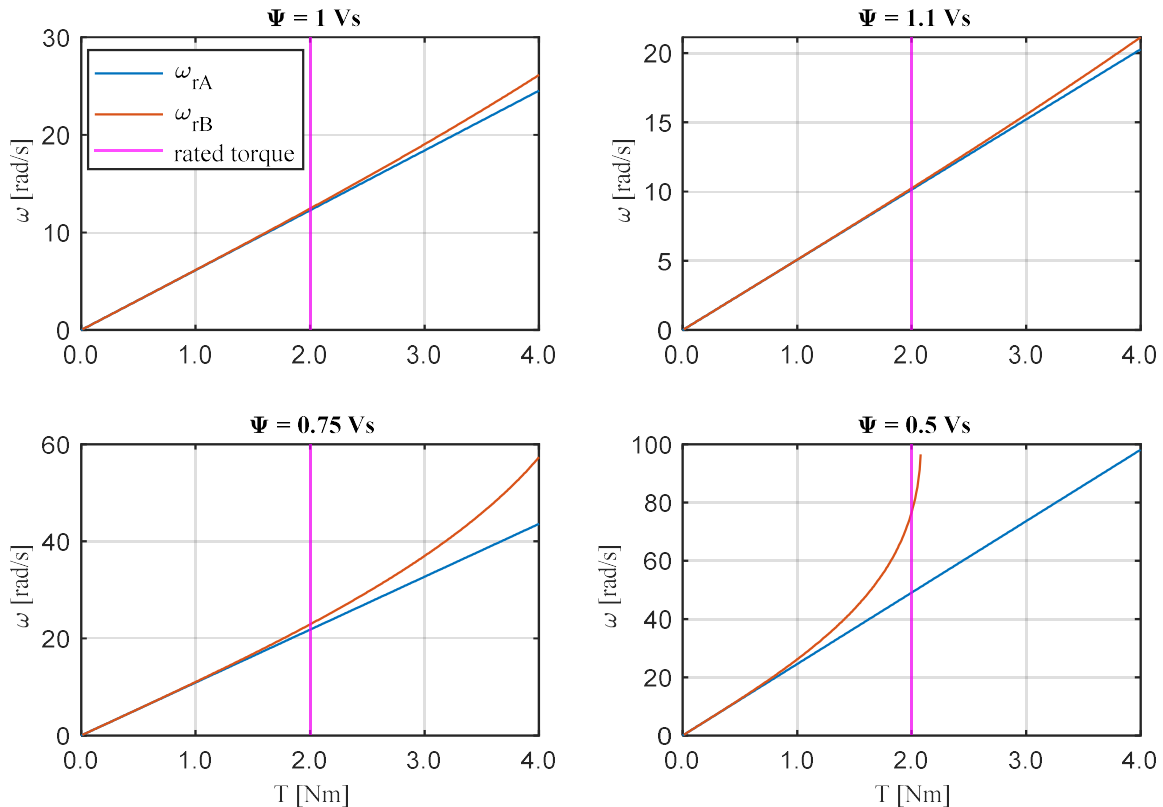


Figure 2: Dependence of rotor frequency on torque at different linkage flux values.

rated. At the linkage flux $\psi = 1.1\text{ Vs}$ the difference is even smaller. On the other hand, when the linkage flux decreases to $\psi = 0.75\text{ Vs}$ and $\psi = 0.5\text{ Vs}$, the difference increases.

Figure 3 shows the rotor current in the d-axis according to the equations (9a) i_{rdA} and (11a) i_{rdB} and the stator current in the q-axis i_{sq} as a function of the torque for four linkage flux values. It can be seen that all rotor d-axis currents i_{rdA} and i_{rdB} and stator q-axis current i_{sq} increase as the linkage flux decreases. The difference between the value of i_{rdA} and i_{rdB} increases with increasing torque. A significant difference occurs at reduced linkage flux, especially at $\psi = 0.5\text{ Vs}$. Furthermore, the stator q-axis current i_{sq} is higher than the rotor d-axis current i_{rdA} and i_{rdB} .

In Figure 4, the stator currents in the d-axis i_{sdA} and i_{sdB} are plotted as a function of torque at four different linkage fluxes. In particular, the magnetizing current i_u is plotted here using equation (3b). The ellipse corresponding to the rated operation condition of the induction machine i_{max} is also plotted in the graph. In this area, the induction motor can operate continuously. For the linkage flux $\psi = 1\text{ Vs}$ and $\psi = 1.1\text{ Vs}$ it can be seen that the difference between the currents i_{sdA} and i_{sdB} is very small. For lower linkage flux $\psi = 0.75\text{ Vs}$ and $\psi = 0.5$, the difference increases, especially at higher torque. The currents i_{sdA} and i_{sdB} are also affected

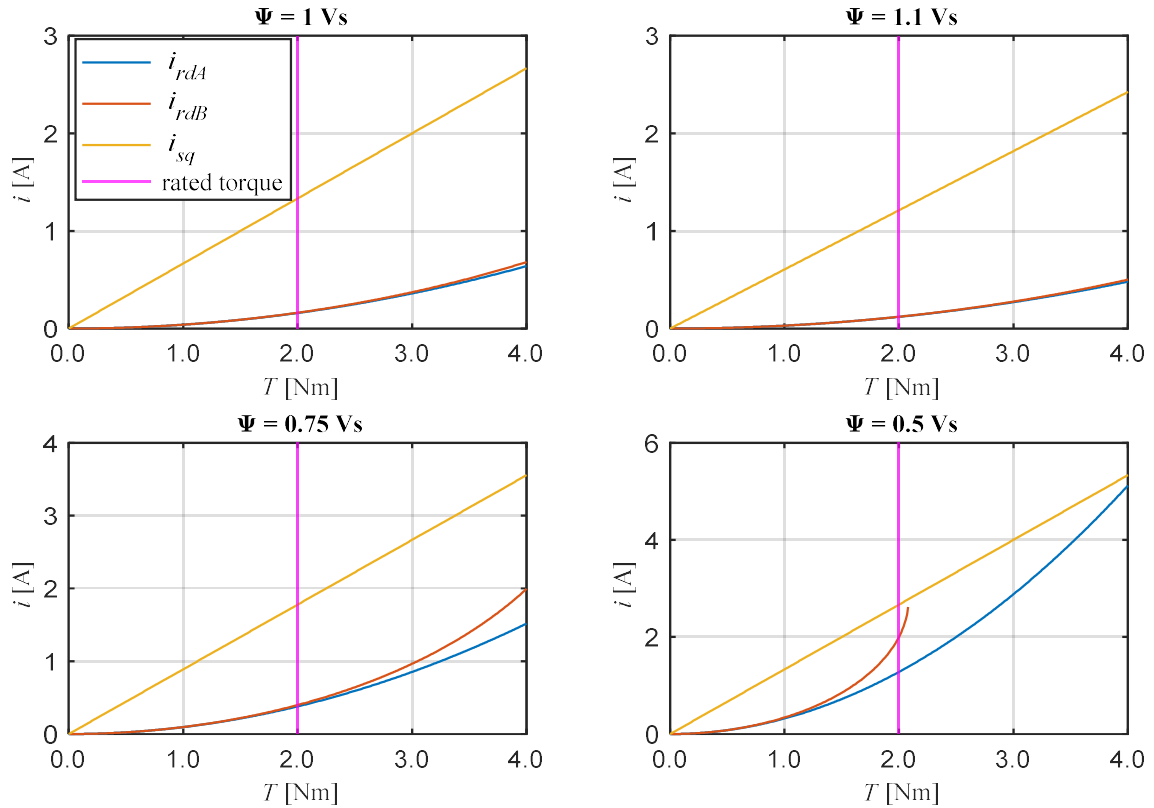


Figure 3: Dependence of rotor currents on torque at different linkage flux values.

by the magnetizing current i_u , which increases with increasing linkage flux. Only at $\psi = 0.5$, the rated torque line passes only with i_{sdB} and not with i_{sdA} .

Figure 5 shows the iron loss P_{Fe} , Joule losses in the rotor winding (P_{jrA} and P_{jrB}) and stator winding (P_{jsA} and P_{jsB}), depending on the torque at different linkage flux values. Losses were calculated by considering

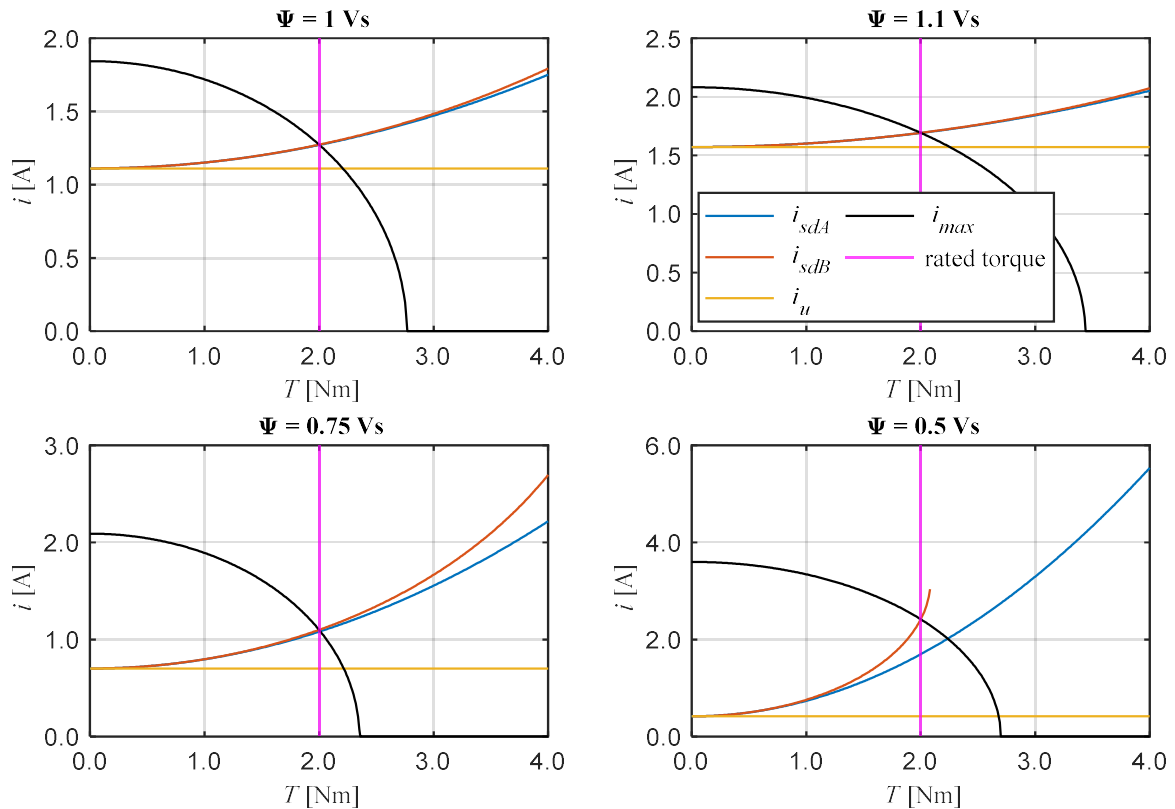


Figure 4: Dependence of stator currents on torque at different linkage flux values.

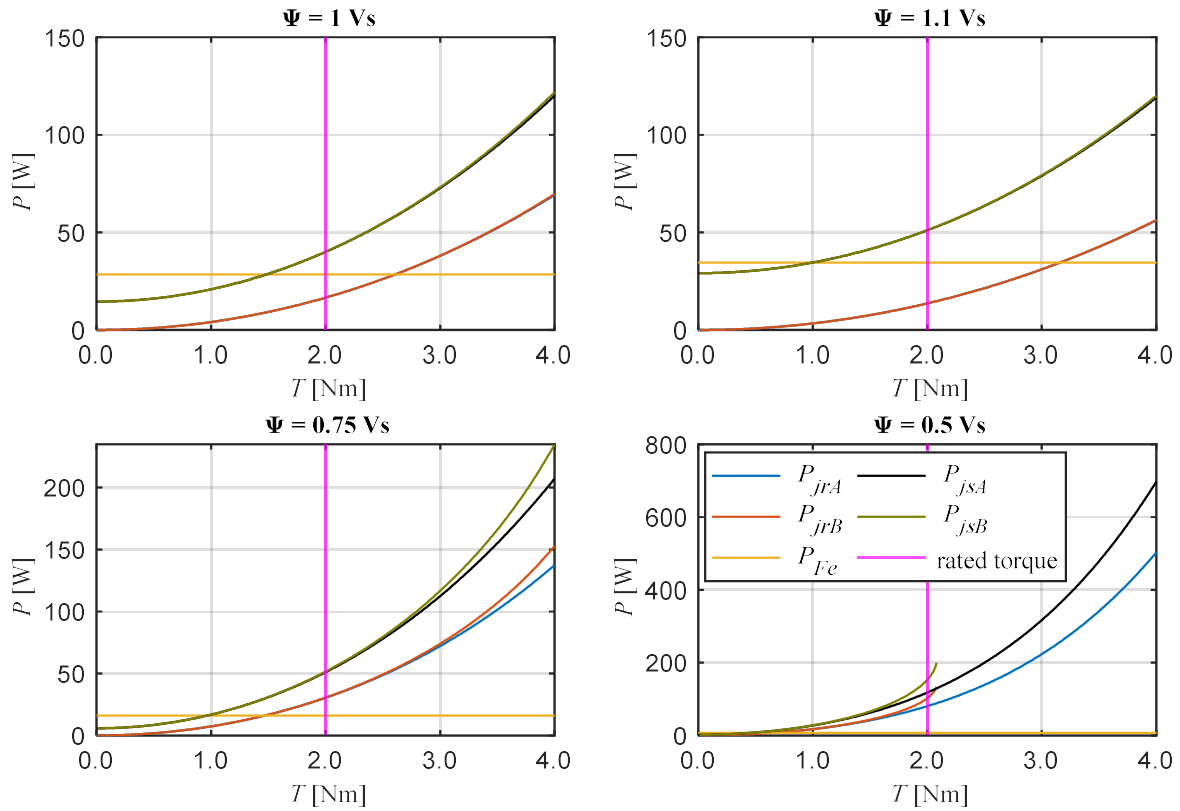


Figure 3: Dependence of power losses on torque at different linkage flux values.

two current values according to equations (9a, b) and (11a, b). It can be seen that the difference between P_{jrA} and P_{jrB} and P_{jsA} and P_{jsB} , respectively, occurs at low value of linkage flux. Furthermore, it can be seen how the iron loss P_{Fe} increases with increasing linkage flux.

6 CONCLUSION

The aim of this paper was to calculate ω_r according to two different formulas and to verify its influence on quantities in the equivalent circuit of the induction machine, especially on current and power losses. It can be seen from Figures 2-5 that at higher linkage flux value, the difference between ω_{rA} (8) and ω_{rB} (10) is negligible. At low flux values, the difference between ω_{rA} and ω_{rB} increases, especially especially at a higher torque value. However, the motor is not expected to operate at rated torque at reduced linkage flux. Thus, the simplified formula for calculating ω_{rA} (8) can be considered sufficient and can be replaced by the natural formula ω_{rB} (10) for the analytical expression of the optimal linkage flux.

ACKNOWLEDGEMENT

This research work has been carried out in the Centre for Research and Utilization of Renewable Energy (CVVOZE). Authors gratefully acknowledge financial support from the Ministry of Education, Youth and Sports under institutional support and BUT specific research programme (project No. FEKT-S-20-6379).

REFERENCES

- [1] M. N. Uddin and S. W. Nam, "New Online Loss-Minimization-Based Control of an Induction Motor Drive," in *IEEE Transactions on Power Electronics*, vol. 23, no. 2, pp. 926-933, March 2008, doi: 10.1109/TPEL.2007.915029.
- [2] N. P. Quang and J. A. Dittich, *Vector Control of Three-Phase AC Machines System Development in the Practice*. Berlin, Germany: Springer-Verlag, 2008.
- [3] M. Toman, R. Cipin, P. Vorel and M. Mach, "Algorithm for IM Optimal Flux Determination Respecting Nonlinearities and Thermal Influences," 2018 IEEE International Conference on Environment and Electrical Engineering and 2018 IEEE Industrial and Commercial Power Systems Europe (EEEIC / I&CPS Europe), Palermo, 2018, pp. 1-5, doi: 10.1109/EEEIC.2018.8493953.